Association of quantitative computed tomography-based right atrial appendage and right atrium parameters with postradiofrequency ablation recurrence of atrial fibrillation

Tong Pan[1,2]^, Yang Liu[1]^, Yang Yu[1]^, Dan Zhang[3]^, Yu-Han Sun[1]^, Hao-Wen Zhang[1]^, Cai-Ying Li[1]^

[1]Department of Medical Imaging, The Second Hospital of Hebei Medical University, Shijiazhuang, China; [2]Department of Radiology, Hebei General Hospital, Shijiazhuang, China; [3]Department of Radiology, The Third Hospital of Hebei Medical University, Shijiazhuang, China

Contributions: (I) Conception and design: T Pan, CY Li; (II) Administrative support: CY Li, Y Liu; (III) Provision of study materials or patients: T Pan, Y Yu, D Zhang; (IV) Collection and assembly of data: YH Sun, HW Zhang; (V) Data analysis and interpretation: T Pan, Y Liu, YH Sun; (VI) Manuscript writing: All authors; (VII) Final approval of manuscript: All authors.

Correspondence to: Cai-Ying Li, MD. Department of Medical Imaging, The Second Hospital of Hebei Medical University, 215 West Heping Road, Shijiazhuang 050000, China. Email: licaiying63@163.com.

Background: The significance of the right atrial appendage (RAA) and right atrium (RA) in the recurrence of atrial fibrillation (AF) after radiofrequency ablation (RFA) remains uncertain. This retrospective case-control study aimed to quantitatively evaluate the role of morphological parameters of the RAA and RA in the recurrence of AF after RFA based on 256-slice spiral computed tomography (CT).

Methods: A total of 297 patients with AF who underwent RFA for the first time between January 1 and October 31, 2020, were enrolled in the study, and they were divided into a nonrecurrence group (n=214) and a recurrence group (n=83). The volume of the RA, RAA and left atrium (LA); height of the RAA; long and short diameter, perimeter, and area of the RAA base; right atrial anteroposterior diameter; tricuspid annulus diameter; crista terminalis thickness; and cavotricuspid isthmus (CVTI) were measured, and the clinical data of patients were collected.

Results: (I) Multivariable logistic regression analysis followed by univariable logistic regression analysis showed that the height of the RAA [odds ratio (OR) =1.124; 95% confidence interval (CI): 1.024–1.233; P=0.014], short diameter of the RAA base (OR =1.247; 95% CI: 1.118–1.391; P=0.001), crista terminalis thickness (OR =1.594; 95% CI: 1.052–2.415; P=0.028) and duration of AF (OR =1.009; 95% CI: 1.003–1.016; P=0.006) were independent predictors of postradiofrequency ablation AF recurrence. (II) Receiver operating characteristic (ROC) curve analysis showed that the prediction model constructed according to the multivariate logistic regression analysis presented good accuracy [area under the curve (AUC) =0.840; P=0.001]. A short diameter of the RAA base >26.95 mm had the highest predictive value for AF recurrence, with a sensitivity of 0.614 and a specificity of 0.822 (AUC =0.786, P=0.001). Pearson correlation analysis showed that there was a significant correlation between right atrial volume and left atrial volume (r=0.720, P<0.001).

Conclusions: A significant increase in diameter and volume of the RAA and RA and tricuspid annulus diameter may correlate with postradiofrequency ablation AF recurrence. The height of the RAA, short diameter of the RAA base, crista terminalis thickness, and AF duration were independent predictors of recurrence. Among them, the short diameter of the RAA base had the highest predictive value for recurrence.

^ ORCID: Tong Pan, 0000-0003-2491-5961; Yang Liu, 0000-0003-2316-9047; Yang Yu, 0000-0002-4348-4418; Dan Zhang, 0000-0002-4250-7550; Yu-Han Sun, 0000-0002-3246-0963; Hao-Wen Zhang, 0000-0002-0456-401X; Cai-Ying Li, 0000-0002-1831-365X.

Introduction

Atrial fibrillation (AF) is one of the most common arrhythmias (1). The age-related increase in AF prevalence and mortality can mostly induce heart failure, stroke, and dementia (2). Radiofrequency ablation (RFA), the first-line treatment for drug-refractory AF (3), can decrease the incidence of thromboembolism and improve clinical symptoms and quality of life. However, the postablation AF recurrence rate is high (accounting for 10–30%) (3), and the etiopathology of AF recurrence is unclear. In recent years, the evaluation of risk factors for postcatheter ablation AF recurrence has become a research topic of interest, and the majority of experimental studies have focused on the left atrium (LA) and pulmonary vein. The LA potentially plays a key role in AF pathophysiology, and factors associated with the LA and left atrial appendage (LAA) are likely predictors of postradiofrequency ablation AF recurrence (4).

With advances in interventional cardiac surgery, the clinical need for an in-depth evaluation of the anatomical structure of the right atrial appendage (RAA) and right atrium (RA) has generated widespread interest. It has been emphasized that the RA volume in AF patients plays a specific role in the recurrence of AF after RFA (5). Some in-depth studies of RAA and RA anatomy and function have been conducted accordingly (6,7). However, clinical studies of the correlation between RAA, RA, and postradiofrequency ablation AF recurrence are relatively limited. Therefore, the role of RAA and RA in recurrence remains unelucidated.

Multiple imaging methods are available to study the morphology and function of the RAA and RA. Echocardiography is the most widely used imaging tool for evaluating cardiac structure in the clinical field. Due to the influence of the chest wall and lung tissue, transthoracic ultrasound cannot be used to observe the RAA. In comparison, transesophageal ultrasound is a semi-invasive examination that is difficult to perform and is easily affected by the operator's experience and equipment, so its accuracy is limited. Cardiovascular magnetic resonance (CMR) is the gold standard for cardiac volume assessment (6) and can provide information about cardiac structure and function (8). However, it is time-consuming and expensive. Cardiac computed tomography (CCT) has the advantages of fast scanning speed, high temporal and spatial resolution, low ionizing radiation and powerful postprocessing function. The use of a double-barrel high-pressure syringe (Stellant) and contrast injection software (P3T software) (9) improved the enhancement of the RAA and RA, which can be used to objectively evaluate right cardiac disease.

This study was conducted with the aim of quantitatively evaluating the anatomical structures of the RAA and RA and other related anatomical structures of patients in the recurrence group and nonrecurrence group and to elucidate the role of the RAA and RA in postradiofrequency ablation AF recurrence. We present the following article in accordance with the STROBE reporting checklist (available at https://qims.amegroups.com/article/view/10.21037/qims-22-951/rc).

Methods

Study design and participants

In this retrospective case-control study, 297 patients with postradiofrequency ablation AF in the Department of Cardiology, The Second Hospital of Hebei Medical University, between January 1 and October 31, 2020, were enrolled. All patients underwent preoperative cardiac computed tomography angiography (CCTA) examination. They were diagnosed by clinical electrocardiogram (ECG) and physical examination. The inclusion criteria were as follows: (I) patients with AF who successfully underwent ablation treatment for AF; (II) patients who had undergone preoperative 256-slice spiral computed tomography (CT); and (III) patients who had no serious postoperative complications that eventually led to death and loss of follow-up (10), including cardiac tamponade, atrioesophageal fistulas, intraprocedural acute myocardial infarction, intra- or postprocedural stroke and extrapericardial bleeding. The exclusion criteria were as follows: (I) poor image quality of CTA resulting in an inability to measure the volume of the
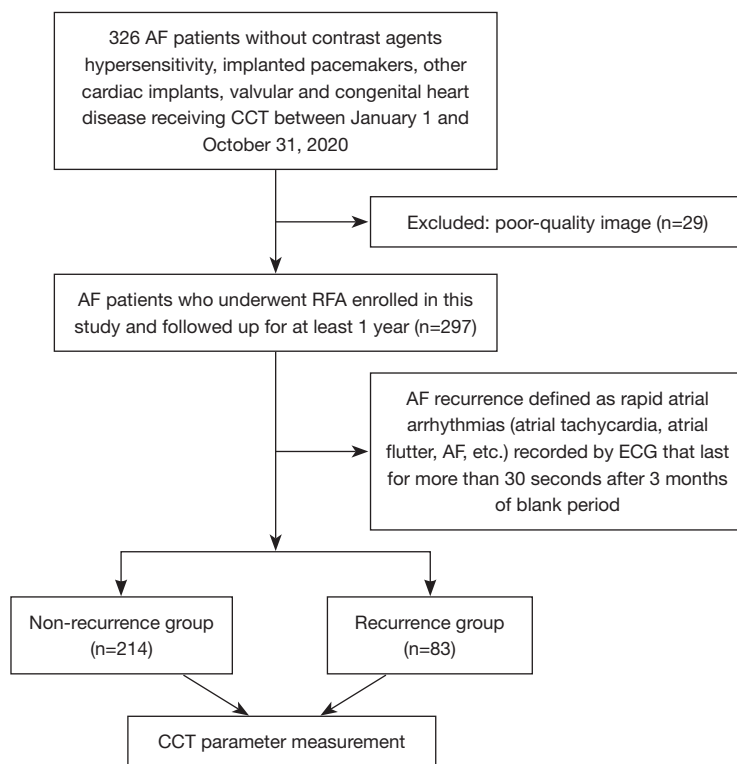
Figure 1 Flow chart of patient enrollment. AF, atrial fibrillation; CCT, cardiac computed tomography; RFA, radiofrequency ablation; ECG, electrocardiogram.

RAA and RA or the thickness of the crista terminalis; (II) contrast agent hypersensitivity, implanted pacemakers, and other cardiac implants; and (III) valvular and congenital heart disease. Valvular heart disease can lead to cardiac remodeling, and it will interfere with AF itself as a research factor affecting the expansion of the RAA and RA. The flowchart for patient enrollment is shown in *Figure 1*.

RFA was performed in the cardiology department according to the unified standard. Before the operation, a multiconductive physiology and Coil-Assisted Retrograde Transvenous Obliteration (CARTO) 3.0 three-dimensional mapping system were connected. Coronary sinus electrodes were inserted into the subclavian vein or femoral vein. Atrial septal puncture was performed to reconstruct the LA and pulmonary veins in three dimensions. Two-way block between the pulmonary veins and LA was confirmed by electrophysiological stimulation after the operation.

Postradiofrequency ablation AF recurrence was defined as rapid atrial arrhythmias (atrial tachycardia, atrial flutter, AF, etc.) recorded by ECG that lasted for more than 30 seconds after a 3-month blank period (3). The patients were followed up for at least 1 year. The recurrence of

AF was evaluated by telephone and outpatient follow-up using surface ECG and 24-hour dynamic ECG at 3, 6 and 12 months, and AF recurrence was considered the endpoint of follow-up. This study was conducted in accordance with the Declaration of Helsinki (as revised in 2013). The study was approved by the Institutional Ethics Committee of The Second Hospital of Hebei Medical University (No. 2018-R245). The institutional review committee waived the requirement for informed consent owing to the retrospective nature of the study.

CCTA technique

CCTA with Phillips 256-slice spiral CT (Brilliance iCT, Philips Health care, Amsterdam, The Netherlands) was performed preoperatively in AF patients in our hospital. Patients were instructed to undergo breath-holding training before the scan. The scan range was from 0.5 cm below the tracheal bifurcation until the diaphragmatic surface of the heart. Using a high-pressure syringe (350 mgI/mL, 0.8 mL/kg), iohexol contrast agent was injected into the median cubital vein at a flow rate of 4–5 mL/s.
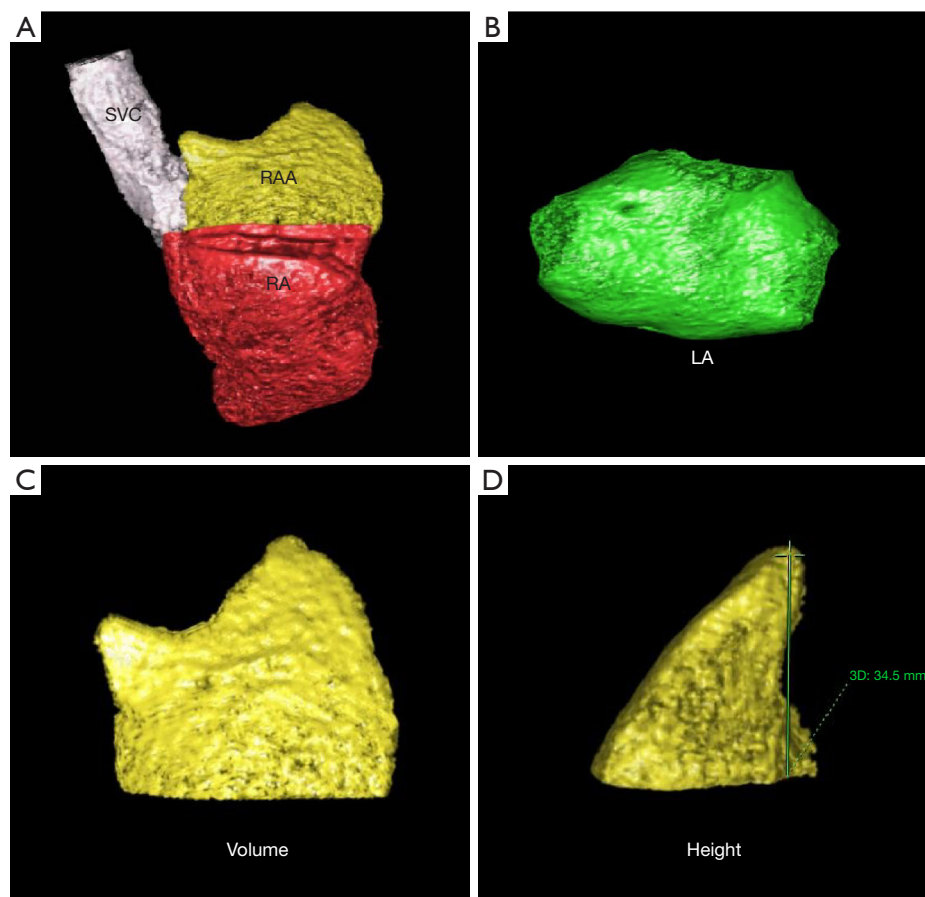
Figure 2 Measurement of the volume of the RAA, RA, and LA and the height of the RAA. (A) Three-dimensional images of the RAA and RA were obtained by cardiac function software. (B) The 3D image of the LA. (C) The volume of RAA was measured. (D) The height of the RAA was measured from the highest point to the base of the RAA. SVC, superior vena cava; RAA, right atrial appendage; RA, right atrium; LA, left atrium; 3D, 3-dimensional.

The scanning parameters were as follows: tube voltage, 80–120 kV; collimation, 128×0.625; pitch, 0.18; matrix, 512×512; tube current, 280–350 mAs/revolution; and rotation time, 330 ms.

Image postprocessing technology and measurement method

On a Philips EBW 4.6 workstation (Philips Healthcare), 75% phase reconstruction of the cardiac cycle was selected for postprocessing. The RAA and RA were reconstructed by volume reproduction (VR) and multiplanar reconstruction (MPR). At the boundary between the RAA and the RAA base, the transition between the superior vena cava (SVC) and the RA was selected as the location of the superior vena caval orifice. The upper boundary was the diameter line of the SVC, and the lower boundary was the RA. The axial

image of the orifice of the SVC was used as the boundary, and the RAA was situated above this level; the RAA was visualized using cardiac function postprocessing software, and 3-dimensional (3D) images of the RAA were obtained. The RAA is a pouch-like structure that projects anteriorly from the RA, and as confirmed previously, the base of the RAA lies perpendicular to the long axis of the RAA (11,12); thus, the RAA base is anatomically located at the superior vena caval orifice.

Measurement methods: (I) volume of the RAA, RA, and LA: 3D images of the RAA, RA, and LA were obtained using heart function analysis software, and the volumes of the RAA, RA, and LA were measured (*Figure 2A-2C*). (II) Height of the RAA: the height from the highest point to the base of the RAA was measured (*Figure 2D*). (III) Measurement of the long and short diameter, perimeter,

3806

Pan et al. Relation of right atrium with atrial fibrillation recurrence
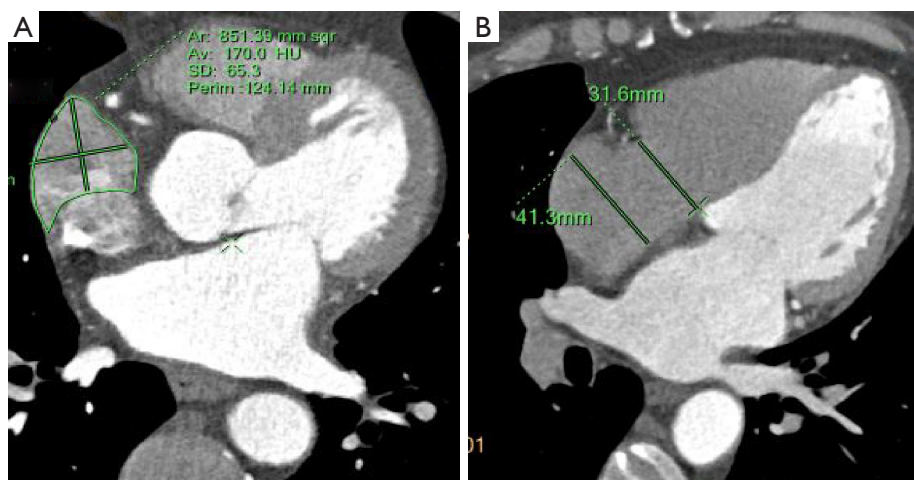
Figure 3 The diameters of the RAA base, the tricuspid annulus and the right atrial anteroposterior diameter were measured. (A) Measurements of the long and short diameters, perimeter, and area of the RAA base were obtained from the level of the superior vena caval orifice on axial images. (B) Measurement of the diameter of the tricuspid annulus and the right atrial anteroposterior diameter at the four-chamber heart level. The right atrial anteroposterior diameter was 41.3 mm, and the diameter of the tricuspid annulus was 31.3 mm, as shown in (B). Ar, area; Av, average; SD, standard deviation; Perim, perimeter; RAA, right atrial appendage.
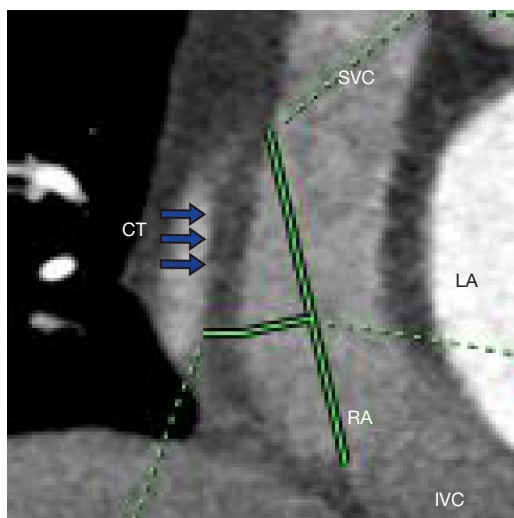
Figure 4 Measurement of the CT thickness: the optimal position of the coronal image was adjusted to show the extension of the CT from the SVC to the IVC; a line was drawn from the right edge of the SVC to the right edge of the IVC, and a vertical line was drawn through the midpoint of this line to intersect the CT; then, the thickness of the CT was measured in this region. CT, crista terminalis; SVC, superior vena cava; LA, left atrium; RA, right atrium; IVC, inferior vena cava.

and area of the RAA base: the base of the RAA is situated at the level of the superior vena caval orifice on axial images, and the measurements of the long diameter, short diameter, perimeter, and area of the RAA base were measured on the axial image (*Figure 3A*). (IV) The RA anteroposterior diameter and the tricuspid annulus diameter were obtained at the four-chamber level (6) (*Figure 3B*). (V) Measurement of crista terminalis thickness (13,14): the optimal position of the coronal image was adjusted to show that the crista terminalis extended from the SVC to the inferior vena cava; a line was drawn from the right edge of the SVC to the right edge of the inferior vena cava, a vertical line was drawn through the midpoint of the line to intersect the crista terminalis, and the thickness of the crista terminalis was measured in this region (*Figure 4*). (VI) Measurement of the cavotricuspid isthmus (CVTI): CVTI includes the paraseptal, central, and lateral isthmus. The paraseptal isthmus was displayed at the four-chamber heart level at the central level of the coronary sinus orifice. The length of the paraseptal isthmus was measured as the distance between the attachment of the tricuspid septum and the Eustachian ridge (ER) (*Figure 5*). The ER is located at the entrance of the inferior vena cava and constitutes the boundary between

the fossa ovalis and the coronary sinus. The central and lateral isthmus were measured from the anterior and lateral edges, respectively, of the inferior vena cava to the tricuspid annulus on the two-chamber views of the right ventricle (*Figure 6A,6B*).

All parameters were analyzed by two experienced radiologists, without knowledge of the patient's clinical data, who reached a consensus on each examination.

Statistical analysis

SPSS version 25.0 (SPSS, Inc., Chicago, IL, USA) was used for data analysis. The normality test using Shapiro-Wilk was conducted for continuous data to determine whether the dataset conformed to a normal distribution. Mean intergroup comparisons with a normal distribution are expressed as the mean ± standard deviation (SD) and were analyzed by the independent sample t-test, whereas data with nonnormal distribution are expressed as the median (interquartile range) and were analyzed by the Wilcoxon rank-sum test. Counting data are expressed as numbers (percentages) and were analyzed with the chi-square test. Univariable and multivariable logistic regression analyses were performed to identify the factors related to AF recurrence in the data with positive results. The collinearity test of variables was included in the model. By calculating different variance inflation factors, strong correlation variables were excluded. The receiver operating characteristic (ROC) curve was used to evaluate the accuracy of the prediction model and variables in predicting recurrence. Pearson correlation analysis was used to analyze the RA and LA volumes. Statistical significance was set at $P < 0.05$.

Figure 5 The length of the paraseptal isthmus is the distance between the attachment of the tricuspid septum and the ER. FOV, field of view; ER, Eustachian ridge.
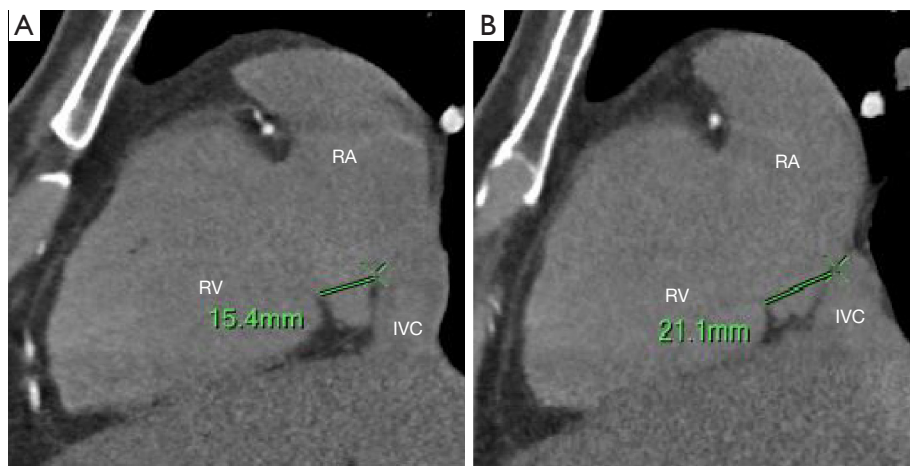
Figure 6 The central and lateral isthmus were measured from the anterior and lateral edges, respectively, of the IVC to the tricuspid annulus at the level of the two-chamber view of the RV. (A) The central isthmus was measured from the anterior edges of the IVC to the tricuspid annulus at the level of the two-chamber view of the RV. (B) The lateral isthmus was measured from the lateral edges of the IVC to the tricuspid annulus at the level of the two-chamber view of the RV. RA, right atrium; RV, right ventricle; IVC, inferior vena cava.

Table 1 Clinical characteristics of the postradiofrequency ablation AF recurrence and AF nonrecurrence groups

Characteristics	AF recurrence (n=83)	AF nonrecurrence (n=214)	P
Sex, males	50 (60.2)	123 (57.5)	0.665
Age (years)	63.07±12.07	60.35±10.58	0.057
BMI (kg/m^2)	25.31 [23.18, 27.64]	25.93 [23.69, 28.04]	0.356
PeAF	30 (36.1)	37 (17.3)	0.001
Heart failure	28 (33.7)	43 (20.1)	0.013
Hypertension	50 (60.2)	115 (53.7)	0.312
Diabetes	21 (25.3)	30 (14.0)	0.021
Coronary heart disease	48 (57.8)	120 (56.1)	0.784
Hyperlipidemia	20 (24.1)	48 (22.4)	0.759
Stroke/TIA	13 (15.7)	38 (17.8)	0.668
CHA2DS2-VASc score	2.89±1.68	2.47±1.52	0.037
AF duration (months)	24 [4, 72]	12 [2, 48]	0.008

Data are presented as the mean ± SD, median [interquartile range], or n (%). AF, atrial fibrillation; BMI, body mass index; PeAF, persistent atrial fibrillation; TIA, transient ischemic attack; SD, standard deviation.

Results

Participant characteristics

During the study period, 326 patients underwent RFA, and 29 patients were excluded due to poor image quality. Among the 297 participants, there were 214 participants (123 men and 91 women) in the AF nonrecurrence group (age 60.35±10.58 years) and 83 (50 men and 33 women) in the AF recurrence group (age 63.07±12.07 years). The comparison of clinical data between the recurrence group and nonrecurrence group showed no significant differences in age; sex; body mass index (BMI); or incidence of hypertension, coronary heart disease, hyperlipidemia, or stroke/transient ischemic attack (TIA) (P>0.05) (*Table 1*). The incidence of diabetes, heart failure, and persistent atrial fibrillation (PeAF); duration of AF; and CHA2DS2-VASc score in the AF recurrence group were significantly higher than those in the AF nonrecurrence group (P<0.05).

Morphological parameters of the RAA, RA and related structures

The RAA volume; short diameter, perimeter, and area of RAA base; RAA height; RA volume; RA anteroposterior diameter; tricuspid annulus diameter; crista terminalis thickness; paraseptal isthmus; central isthmus; lateral isthmus; right atrial volume index (RAVI); left atrial

volume index (LAVI); and LA volume were quantified by 256-slice spiral CT postprocessing of cardiac function. Comparison of the CT-related parameters of the RAA and RA between the postradiofrequency ablation AF recurrence and nonrecurrence groups showed that all parameters in the AF recurrence group were higher than those in the nonrecurrence group (all P<0.05) (*Table 2*). There were no significant differences in the long diameter of the RAA base between the AF recurrence group and the AF nonrecurrence group.

Univariable logistic regression analysis showed that RAA volume; short diameter, perimeter, and area of RAA base; RAA height; right atrial volume; right atrial anteroposterior diameter; tricuspid annulus diameter; crista terminalis thickness; paraseptal isthmus; central isthmus; lateral isthmus; RAVI; LAVI; left atrial volume; PeAF; CHA2DS2-VASc score; AF duration; heart failure; and diabetes were significant (P<0.05) risk factors for AF recurrence after RFA (*Table 3*). The following variance inflation factors were greater than 10 in the regression model: left atrial volume (229.035), RAVI (219.312), area of RAA base (29.430) and LAVI (224.081). Due to multicollinearity, these variables were excluded. The variance inflation factors of the other variables were less than 10 and could be used for multivariable logistic regression analysis.

Multivariable logistic regression analysis showed that the short diameter of the RAA base, RAA height, crista

Table 2 Comparison of the CT-related parameters of the RAA and RA between the postradiofrequency ablation AF recurrence and AF nonrecurrence groups

CT-related parameters	AF recurrence (n=83)	AF nonrecurrence (n=214)	P value
RAA volume (mL)	12.20 (9.80, 16.10)	8.4 (6.40, 11.20)	0.001
RAA height (mm)	29.98±5.09	26.02±5.09	0.001
RAA base			
Long diameter (mm)	36.51±5.48	35.18±5.54	0.063
Short diameter (mm)	28.21±5.22	22.41±5.21	0.001
Area (mm^2)	832.70 (714.26, 1,062.38)	672.42 (579.03, 794.57)	0.001
Perimeter (mm)	117.56±15.31	106.20±13.65	0.001
RA volume (mL)	92.19±33.94	76.46±20.22	0.001
RA anteroposterior diameter (mm)	47.40 (44.10, 53.00)	45.50 (41.90, 48.55)	0.001
Tricuspid annulus diameter (mm)	38.87±5.02	36.22±5.31	0.001
RAVI (mL/m^2)	47.69 (37.83, 65.02)	41.99 (35.91, 49.63)	0.001
Paraseptal isthmus (mm)	16.10 (14.70, 17.20)	15.70 (14.68, 16.40)	0.020
Central isthmus (mm)	21.66±3.66	19.28±3.01	0.001
Lateral isthmus (mm)	25.70±4.62	23.14±3.47	0.001
Crista terminalis thickness (mm)	3.70 (3.30, 4.40)	3.40 (3.10, 3.90)	0.001
LA volume (mL)	115.15±40.39	93.13±25.02	0.001
LAVI (mL/m^2)	62.12 (48.19, 78.57)	52.37 (42.99, 61.76)	0.001

Data are presented as the mean ± SD or median (interquartile range). CT, computed tomography; RAA, right atrial appendage; RA, right atrium; AF, atrial fibrillation; RAVI, right atrial volume index; LA, left atrium; LAVI, left atrial volume index.

terminalis thickness, and duration of AF were independent predictors of postradiofrequency ablation AF recurrence (*Table 4*) (P<0.05).

Predictive value of parameters

Multivariable logistic regression analysis was used to construct the prediction model (*Figure 7*), and the ROC curve was drawn using the predicted P value [area under the curve (AUC) =0.840, P=0.001, standard error 0.024, 95% confidence interval (CI): 0.793–0.888]; the optimal cutoff P value was 0.276, and the corresponding sensitivity and specificity were 0.795 and 0.748, respectively. ROC curves were drawn for the short diameter of the RAA base, RAA height, crista terminalis thickness and AF duration. Short diameter of the RAA base >26.95 mm (sensitivity, 0.614; specificity, 0.822; AUC, 0.786; P=0.001), RAA height >27.85 mm (sensitivity, 0.880; specificity, 0.467; AUC, 0.718; P=0.001), crista terminalis thickness >3.65 mm (sensitivity, 0.590; specificity, 0.654; AUC, 0.643; P=0.001),

and AF duration >13.5 months (sensitivity, 0.627; specificity, 0.547; AUC, 0.607; P=0.004) had the highest predictive value for AF recurrence after RFA (*Table 5, Figure 8*).

Correlation between RA volume and LA volume

Pearson correlation analysis showed a significant correlation between the RA and LA volumes (*Figure 9*; r=0.720, P<0.001, 95% CI: 0.661–0.771).

Discussion

RFA is an effective treatment for AF. However, the high postoperative recurrence rate constitutes a difficult problem in current AF treatment (15). Therefore, effective identification of risk factors for postradiofrequency ablation AF recurrence is crucial for adjusting the postoperative treatment for AF patients, and close follow up of patients who are prone to AF recurrence is very important (16).

The results of this study showed that diabetes, heart

3810

Pan et al. Relation of right atrium with atrial fibrillation recurrence

Table 3 Univariable regression analysis of variables with AF recurrence

Variables	OR (95% CI)	P value
RAA volume	1.211 (1.138–1.289)	0.001
RAA height	1.153 (1.094–1.215)	0.001
Short diameter of RAA base	1.225 (1.157–1.297)	0.001
Area of RAA base	1.004 (1.003–1.005)	0.001
Perimeter of RAA base	1.056 (1.036–1.077)	0.001
RA volume	1.024 (1.013–1.034)	0.001
RA anteroposterior diameter	1.101 (1.049–1.154)	0.001
Tricuspid annulus diameter	1.105 (1.049–1.164)	0.001
RAVI	1.042 (1.023–1.062)	0.001
Crista terminalis thickness	1.866 (1.331–2.615)	0.001
Paraseptal isthmus	1.251 (1.077–1.452)	0.003
Central isthmus	1.242 (1.144–1.349)	0.001
Lateral isthmus	1.183(1.103–1.270)	0.001
LA volume	1.023 (1.014–1.032)	0.001
LAVI	1.040 (1.023-1.057)	0.001
PeAF	2.708 (1.530–4.793)	0.001
CHA2DS2-VASc score	1.187 (1.009–1.396)	0.038
AF duration	1.007 (1.002–1.012)	0.006
Heart failure	2.025 (1.151–3.561)	0.014
Diabetes	2.077(1.109–3.891)	0.022

AF, atrial fibrillation; OR, odds ratio; CI, confidence interval; RAA, right atrial appendage; RA, right atrium; RAVI, right atrial volume index; LA, left atrium; LAVI, left atrial volume index; PeAF, persistent atrial fibrillation.

Table 4 Multivariable logistic regression analysis of variables with AF recurrence

Variables	OR (95% CI)	P value
RAA volume	0.882 (0.745–1.044)	0.144
RAA height	1.124 (1.024–1.233)	0.014
Short diameter of RAA base	1.247 (1.118–1.391)	0.001
Perimeter of RAA base	0.992 (0.950–1.036)	0.719
RA volume	1.011 (0.991–1.031)	0.289
RA anteroposterior diameter	0.963 (0.894–1.038)	0.330
Tricuspid annulus diameter	1.033 (0.945–1.129)	0.473
Crista terminalis thickness	1.594 (1.052–2.415)	0.028
Paraseptal isthmus	1.014 (0.824–1.249)	0.894
Central isthmus	1.142 (0.964–1.353)	0.123
Lateral isthmus	0.973 (0.837–1.130)	0.720
PeAF	1.259 (0.551–2.876)	0.585
CHA2DS2-VASc score	1.164 (0.917–1.477)	0.211
AF duration	1.009 (1.003–1.016)	0.006
Heart failure	1.213 (0.550–2.675)	0.632
Diabetes	1.062 (0.455–2.479)	0.889

AF, atrial fibrillation; OR, odds ratio; CI, confidence interval; RAA, right atrial appendage; RA, right atrium; PeAF, persistent atrial fibrillation.

failure, PeAF, long duration of AF, and an increased CHA2DS2-VASc score can increase the postradiofrequency ablation AF recurrence rate, which is in agreement with the findings of some previous studies (17,18). Ectopic pacemakers in patients with AF mainly originate in the pulmonary vein, and pulmonary vein isolation is the cornerstone of catheter ablation (19). Therefore, the risk predictors of postradiofrequency ablation AF recurrence in previous studies were mostly concentrated in the LA, LAA, and pulmonary vein (20,21). Santangeli *et al.* noted that the incidence of extrapulmonary venous triggered lesions in patients with AF was 11%, and the common sites were the crista terminalis, SVC, RAA, and LAA (22). With the

Figure 7 ROC curve of the logistic regression model analysis for prediction of postradiofrequency-ablation AF recurrence. ROC, receiver operating characteristic; AUC, area under the curve; CI, confidence interval; AF, atrial fibrillation.

Table 5 ROC curve estimates of the accuracy of variables in predicting recurrence

Variables	AUC	P value	Optimal cutoff P value	Sensitivity	Specificity
Prediction model	0.840	0.001	0.276	0.795	0.748
Short diameter of RAA base	0.786	0.001	26.95	0.614	0.822
RAA height	0.718	0.001	27.85	0.880	0.467
Crista terminalis thickness	0.643	0.001	3.65	0.590	0.654
AF duration	0.607	0.004	13.5	0.627	0.547

ROC, receiver operating characteristic; AUC, area under the curve; RAA, right atrial appendage; AF, atrial fibrillation.
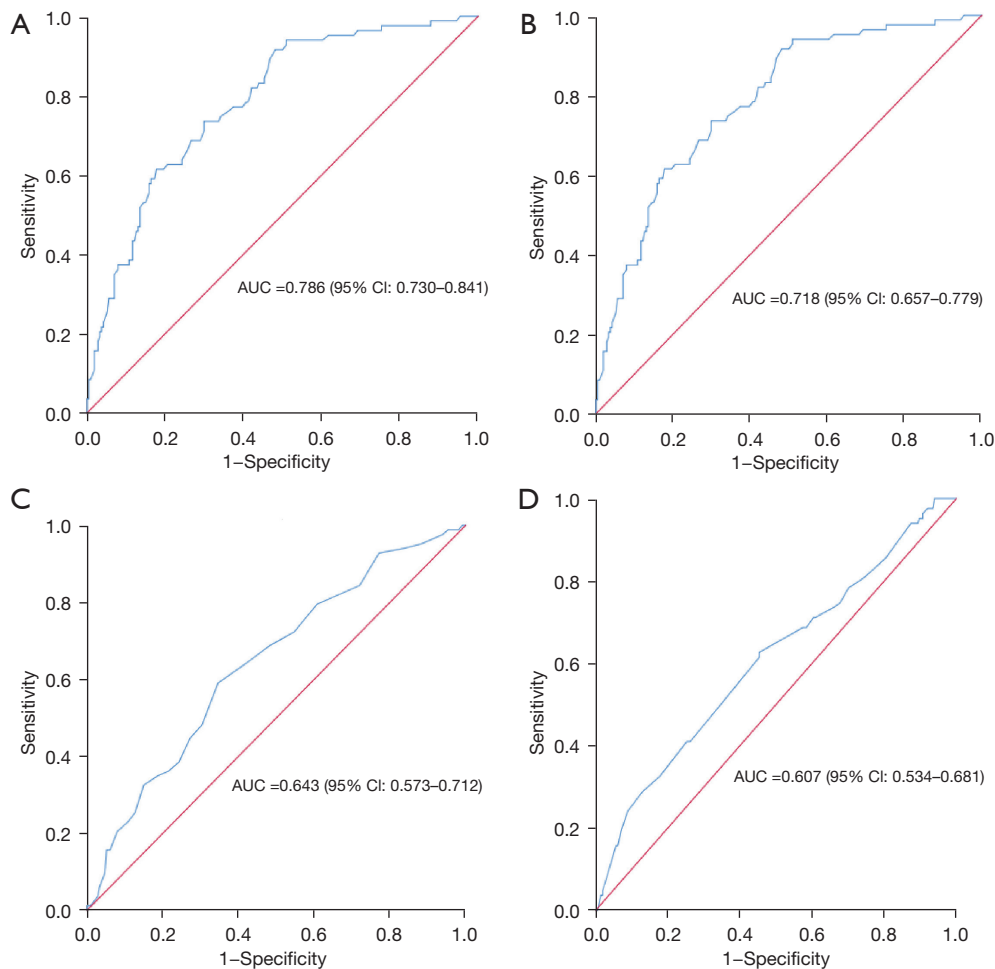
Figure 8 ROC curve analysis of the variables in predicting AF recurrence: short diameter of RAA base ROC curve (A), RAA height ROC curve (B), crista terminalis thickness ROC curve (C), AF duration ROC curve (D). AUC, area under the curve; CI, confidence interval; ROC, receiver operating characteristic; RAA, right atrial appendage; AF, atrial fibrillation.

prolongation of the AF duration, the number of AF-driving foci will increase significantly, and extrapulmonary venous trigger lesions will also increase significantly. The longer the duration of AF in patients with PeAF, the more likely it is that the driving factors of AF would appear in the RAA, RA, and other regions. Therefore, more attention should

3812

Pan et al. Relation of right atrium with atrial fibrillation recurrence
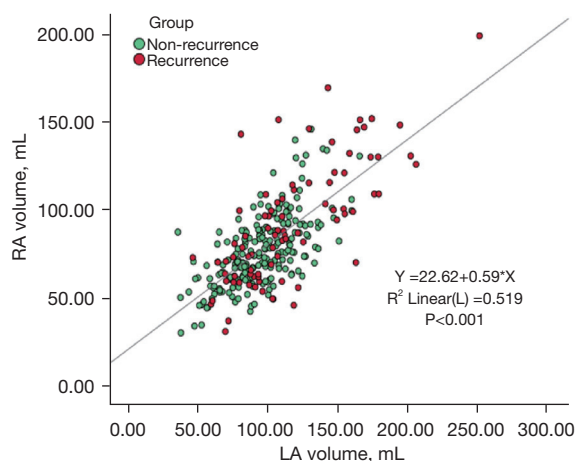
Figure 9 Results of the Pearson correlation analysis of RA and LA volumes. RA, right atrium; LA, left atrium.

be given to the RAA, RA, and related anatomy, especially in patients with PeAF and postoperative AF recurrence.

Some studies have shown that AF and right heart dysfunction can coexist (6,7), and the incidence of AF in patients with right heart dysfunction is as high as 66%. Moon *et al.* noted that the enlargement of the RA was an independent predictor of early postradiofrequency ablation AF recurrence (5), and some authors have proposed that the RA anteroposterior diameter would be reduced after ablation in both the recurrence and nonrecurrence groups (7). This indicates that the RA has better compliance and is more sensitive to hemodynamic changes. A large number of studies on atrial anatomical remodeling have confirmed the relationship between atrial enlargement and AF, but there are limited data on the structure and remodeling of the RAA and RA. Through this study, we ascertained that the RAA volume; short diameter, perimeter, and area of the RAA base; RAA height; RA volume; RA anteroposterior diameter; crista terminalis thickness; paraseptal isthmus; central isthmus; lateral isthmus; RAVI; LAVI; and LA volume in the AF recurrence group were higher than those in the AF nonrecurrence group (P<0.05), which indicates that AF patients with larger RAA and RA diameters are more likely to relapse postoperatively. Close follow-up and timely adjustment of treatment measures should be carried out for these patients. Some studies have shown that the tricuspid annulus diameter can more reliably reflect an AF patient's condition (23,24). In this study, the tricuspid annulus diameter measured in the AF recurrence group was larger than that in the nonrecurrence group, and the difference was statistically significant (P<0.05). The results

indicate that the tricuspid annulus diameter is of great significance for patients with AF who undergo RFA.

The success of RFA requires an excellent knowledge of RA anatomy. The RA is located above the right ventricle and anterolateral to the LA. Three key structures of the RA were studied: the RAA, the crista terminalis, and the CVTI. The RAA is one of the important anatomical landmarks of the RA. The RAA wall is thin, the base is broad, the external surface is relatively flat, and it contains intricately crossed pectinate muscles (25). Permanent atrial pacing usually places a lead in the RAA, which is closely related to the aorta, and iatrogenic aortic perforation should be prevented (26). The crista terminalis is a muscular eminence from the front of the superior vena cava orifice to the front of the inferior vena cava orifice (5,13), which is the boundary between the proper atrium and the vena cava sinus. The crista terminalis is one of the most common sources of focal right atrial arrhythmias (27) and plays an important role in RFA. The CVTI is the part of the right atrial cavity located between the inferior vena cava and the tricuspid valve, which is divided into the paraseptal isthmus, central isthmus, and lateral isthmus (6,13). This region is the target of catheter ablation for the clinical treatment of atrial flutter. Multivariate logistic regression analysis showed that the short diameter of the RAA base, RAA height, crista terminalis thickness and duration of AF were independent predictors of AF recurrence after RFA (P<0.05). Especially when the short diameter of the RAA base is >26.95 mm, the recurrence rate is significantly increased. Thus, the severity of atrial anatomical remodeling is also related to the short diameter of the RAA base, RAA height, crista terminalis thickness, and duration of AF. It is well known that the LA volume is an independent predictor of AF recurrence after RFA (28,29). As shown in the results, there was a significant correlation between the left and right atrial volumes (r=0.720, P<0.001), and the close relationship between the two atrial volumes may be the reason why atrial volume cannot independently predict AF recurrence after RFA, which is consistent with the report by Moon *et al.* (5).

Limitations

This was a retrospective study, and the patients with AF undergoing RFA were all examined by routine cardiac CTA before the operation; thus, the triphasic contrast bolus admixture protocol at a specific injection rate and total contrast volume (9,23) was not used to better visualize the structure of the right heart. Patients with poor image quality were not

included in the study, thus decreasing the sample size. During the study period, 326 patients underwent RFA, and 29 patients were excluded due to poor image quality, which might, with the small sample size, lead to selection bias. Second, the follow-up time was relatively short, which may lead to an underestimation of the AF recurrence rate after RFA.

Conclusions

In summary, the short diameter of the RAA base, RAA height, crista terminalis thickness and duration of AF are independent predictors of postradiofrequency ablation AF recurrence. There was a significant correlation between left and right atrial volumes. In addition, AF patients with larger anatomical diameters of the RAA and RA and larger tricuspid annulus diameters are more likely to experience AF relapse after surgery, which can provide a certain reference value for RFA of AF.

Acknowledgments

Footnote

Reporting Checklist: The authors have completed the STROBE reporting checklist. Available at https://qims.amegroups.com/article/view/10.21037/qims-22-951/rc

Conflicts of Interest: All authors have completed the ICMJE uniform disclosure form (available at https://qims.amegroups.com/article/view/10.21037/qims-22-951/coif). The authors have no conflicts of interest to declare.

Ethical Statement: The authors are accountable for all aspects of the work and ensuring that questions related to the accuracy or integrity of any part of the work are appropriately investigated and resolved. This study was conducted in accordance with the Declaration of Helsinki (as revised in 2013). The study was approved by the Institutional Ethics Committee of The Second Hospital of Hebei Medical University (No. 2018-R245). The institutional review committee waived the requirement for informed consent owing to the retrospective nature of the study.

Open Access Statement: This is an Open Access article distributed in accordance with the Creative Commons

References

1. Habibi M, Calkins H. Atrial fibrillation catheter ablation: an updated review of current guidelines and expert consensus documents. Herzschrittmacherther Elektrophysiol 2019;30:371-6.

2. Iwayama T, Arimoto T, Ishigaki D, Hashimoto N, Kumagai YU, Koyama YO, Kiribayashi N, Netsu S, Nishiyama S, Takahashi H, Shishido T, Miyamoto T, Sato T, Watanabe T, Kubota I. The Clinical Value of Nongated Dual-Source Computed Tomography in Atrial Fibrillation Catheter Ablation. J Cardiovasc Electrophysiol 2016;27:34-40.

3. Tian X, Zhang XJ, Yuan YF, Li CY, Zhou LX, Gao BL. Morphological and functional parameters of left atrial appendage play a greater role in atrial fibrillation relapse after radiofrequency ablation. Sci Rep 2020;10:8072.

4. Simon J, El Mahdiui M, Smit JM, Száraz L, van Rosendael AR, Herczeg S, Zsarnóczay E, Nagy AI, Kolossváry M, Szilveszter B, Szegedi N, Nagy KV, Tahin T, Gellér L, van der Geest RJ, Bax JJ, Maurovich-Horvat P, Merkely B. Left atrial appendage size is a marker of atrial fibrillation recurrence after radiofrequency catheter ablation in patients with persistent atrial fibrillation. Clin Cardiol 2022;45:273-81.

5. Moon J, Hong YJ, Shim J, Hwang HJ, Kim JY, Pak HN, Lee MH, Joung B. Right atrial anatomical remodeling affects early outcomes of nonvalvular atrial fibrillation after radiofrequency ablation. Circ J 2012;76:860-7.

6. Lang RM, Cameli M, Sade LE, Faletra FF, Fortuni F, Rossi A, Soulat-Dufour L. Imaging assessment of the right atrium: anatomy and function. Eur Heart J Cardiovasc Imaging 2022;23:867-84.

7. Wen S-, Liu N, Bai R, Tang RB, Yu RH, Long DY, Sang CH, Jiang CX, Li SN, Wu JH, Ruan YF, Hu R, Du X, Liu XH, Dong JZ, Ma CS. Right atrial diameter and outcome of catheter ablation of atrial fibrillation. J Interv Card Electrophysiol 2017;49:157-64.

8. Benjamin MM, Moulki N, Waqar A, Ravipati H, Schoenecker N, Wilber D, Kinno M, Rabbat M,

3814

Pan et al. Relation of right atrium with atrial fibrillation recurrence

Sanagala T, Syed MA. Association of left atrial strain by cardiovascular magnetic resonance with recurrence of atrial fibrillation following catheter ablation. J Cardiovasc Magn Reson 2022;24:3.

9. Mihl C, Kok M, Altintas S, Kietselaer BL, Turek J, Wildberger JE, Das M. Evaluation of individually body weight adapted contrast media injection in coronary CT-angiography. Eur J Radiol 2016;85:830-6.

10. Deshmukh A, Patel NJ, Pant S, Shah N, Chothani A, Mehta K, Grover P, Singh V, Vallurupalli S, Savani GT, Badheka A, Tuliani T, Dabhadkar K, Dibu G, Reddy YM, Sewani A, Kowalski M, Mitrani R, Paydak H, Viles-Gonzalez JF. In-hospital complications associated with catheter ablation of atrial fibrillation in the United States between 2000 and 2010: analysis of 93 801 procedures. Circulation 2013;128:2104-12.

11. Shinoda K, Hayashi S, Fukuoka D, Torii R, Watanabe T, Nakano T. Structural Comparison between the Right and Left Atrial Appendages Using Multidetector Computed Tomography. Biomed Res Int 2016;2016:6492183.

12. Li CY, Gao BL, Pan T, Xiang C, Zhang XJ, Liu XW, Fan QY. Quantitative analysis of the right auricle with 256-slice computed tomography. Surg Radiol Anat 2017;39:383-91.

13. Siddiqui AU, Daimi SR, Gandhi KR, Siddiqui AT, Trivedi S, Sinha MB, Rathore M. Crista terminalis, musculi pectinati, and taenia sagittalis: anatomical observations and applied significance. ISRN Anat 2013;2013:803853.

14. Morris GM, Segan L, Wong G, Wynn G, Watts T, Heck P, Walters TE, Nisbet A, Sparks P, Morton JB, Kistler PM, Kalman JM. Atrial Tachycardia Arising From the Crista Terminalis, Detailed Electrophysiological Features and Long-Term Ablation Outcomes. JACC Clin Electrophysiol 2019;5:448-58.

15. Li X, Chen Y, Chen G, Deng C, Tang C, Zhang J. Single ring isolation of pulmonary veins combined with electrical isolation of the superior vena cava in patients with paroxysmal atrial fibrillation. Front Cardiovasc Med 2023;9:1028053.

16. Hindricks G, Potpara T, Dagres N, Arbelo E, Bax JJ, Blomström-Lundqvist C, et al. 2020 ESC Guidelines for the diagnosis and management of atrial fibrillation developed in collaboration with the European Association for Cardio-Thoracic Surgery (EACTS): The Task Force for the diagnosis and management of atrial fibrillation of the European Society of Cardiology (ESC) Developed with the special contribution of the European Heart Rhythm Association (EHRA) of the ESC. Eur Heart J 2021;42:373-498.

17. Jaakkola S, Paana T, Airaksinen J, Sipilä J, Kytö V. Association of CHA2DS2-VASc Score with Long-Term Incidence of New-Onset Atrial Fibrillation and Ischemic Stroke after Myocardial Infarction. J Clin Med 2022;11:7090.

18. Liu XW, Tian X, Hu J, Ma GJ, Gao BL, Li CY. Factors associated with left atrial appendage filling defects on early-phase cardiac computed tomography in patients with nonvalvular atrial fibrillation: a case-control study. Quant Imaging Med Surg 2023;13:720-34.

19. Yubing W, Yanping X, Zhiyu L, Weijie C, Li S, Huaan D, Peilin X, Zengzhang L, Yuehui Y. Long-term outcome of radiofrequency catheter ablation for persistent atrial fibrillation. Medicine (Baltimore) 2018;97:e11520.

20. Chou CC, Lee HL, Chang PC, Wo HT, Wen MS, Yeh SJ, Lin FC, Hwang YT. Left atrial emptying fraction predicts recurrence of atrial fibrillation after radiofrequency catheter ablation. PLoS One 2018;13:e0191196.

21. Tian X, Wang C, Gao D, Gao BL, Li CY. Morphological changes in the orifices of the left atrial appendage and left atrium in patients with atrial fibrillation. Quant Imaging Med Surg 2022;12:5371-82.

22. Santangeli P, Marchlinski FE. Techniques for the provocation, localization, and ablation of non-pulmonary vein triggers for atrial fibrillation. Heart Rhythm 2017;14:1087-96.

23. Khalique OK, Cavalcante JL, Shah D, Guta AC, Zhan Y, Piazza N, Muraru D. Multimodality Imaging of the Tricuspid Valve and Right Heart Anatomy. JACC Cardiovasc Imaging 2019;12:516-31.

24. Lim B, Park JW, Hwang M, Ryu AJ, Kim IS, Yu HT, Joung B, Shim EB, Pak HN. Electrophysiological significance of the interatrial conduction including cavo-tricuspid isthmus during atrial fibrillation. J Physiol 2020;598:3597-612.

25. Kamiński R, Grzybiak M, Nowicka E, Kosiński A, Lewicka E, Dąbrowska-Kugacka A, Kozłowski D. Macroscopic morphology of right atrial appendage in humans. Kardiol Pol 2015;73:183-7.

26. Zoppo F, Rizzo S, Corrado A, Bertaglia E, Buja G, Thiene G, Basso C. Morphology of right atrial appendage for permanent atrial pacing and risk of iatrogenic perforation of the aorta by active fixation lead. Heart Rhythm 2015;12:744-50.

27. Faletra FF, Muzzarelli S, Dequarti MC, Murzilli R, Bellu R, Ho SY. Imaging-based right-atrial anatomy by computed tomography, magnetic resonance imaging, and three-dimensional transoesophageal echocardiography:

correlations with anatomic specimens. Eur Heart J Cardiovasc Imaging 2013;14:1123-31.

28. Zhou XJ, Zhang LX, Xu J, Zhu HJ, Chen X, Wang XQ, Zhao M. Establishment and evaluation of a nomogram prediction model for recurrence risk of atrial fibrillation patients after radiofrequency ablation. Am J Transl Res 2021;13:10641-8.

29. Dhillon GS, Honarbakhsh S, Graham A, Ahluwalia N, Abbas H, Welch S, Daw H, Chow A, Earley MJ, Providencia R, Schilling RJ, Lambiase PD, Hunter RJ. Driver characteristics associated with structurally and electrically remodeled atria in persistent atrial fibrillation. Heart Rhythm O2 2022;3:631-8.